



A comparative multi-reference configuration interaction study of the low-lying states of two thione isomers of thiophenol.

Journal:	<i>International Journal of Quantum Chemistry</i>
Manuscript ID	QUA-2020-0067.R1
Wiley - Manuscript type:	Full Paper
Date Submitted by the Author:	n/a
Complete List of Authors:	de Lima, Fillipe; Universidade Federal da Paraiba, Departamento de Química Pereira Rodrigues, Gessenildo; Universidade Federal da Paraíba, Departamento de Química Lucena Jr., Juracy; Universidade Estadual da Paraíba, química Do Monte, Elizete Ventura; Universidade Federal da Paraíba, Departamento de Química Fausto, Rui; Universidade de Coimbra, química Reva, Igor; University of Coimbra, Department of Chemistry do Monte, Silmar; Universidade Federal da Paraíba, Departamento de Química; Universidade Federal da Paraiba, Química
Keywords:	multi-reference configuration interaction, thione isomers of thiophenol, excited states

SCHOLARONE™
Manuscripts

A comparative multi-reference configuration interaction study of the low-lying states of two thione isomers of thiophenol

Filipe Belarmino de Lima,¹ Gessenildo Pereira Rodrigues,² Juracy Regis de Lucena Junior,³ Elizete Ventura,¹ Rui Fausto,⁴ Igor Reva,^{4*} Silmar Andrade do Monte^{1*}

¹Departamento de Química, CCEN, Universidade Federal da Paraíba, 58059-900, João Pessoa-PB, Brazil

²Faculdade Reboças, 58406-040, Campina Grande-PB, Brazil

³Departamento de Química, Universidade Estadual da Paraíba, 58429-500, Campina Grande-PB, Brazil

⁴CQC-Departamento de Química, Universidade de Coimbra, 3004-535, Coimbra, Portugal

*Corresponding authors: reva@qui.uc.pt, silmar@quimica.ufpb.br

Abstract. Multi-reference configuration interaction, MR-CI (including extensivity corrections, named +Q) calculations have been performed on S_0 to S_3 states of cyclohexa-2,4-diene-1-thione (thione **24**) and cyclohexa-2,5-diene-1-thione (thione **25**), which are thione isomers of thiophenol. Several types of uncontracted MR-CIS and MR-CISD wavefunctions have been employed, comprising MR-CI expansions as large as $\sim 365 \times 10^6$ configuration state functions. The nature of the studied excited states has been characterized. Vertical excitation energies (ΔE) and oscillator strengths (f) have been computed. The most intense transitions ($S_0 \rightarrow S_2$ for **24** and $S_0 \rightarrow S_3$ for **25**) do not change with the wavefunction, although a variation as large as ~ 1 eV has been obtained for the S_3 state of **24**, at the highest (MR-CI+Q) level. On the other hand, ΔE changes at most ~ 0.56 eV for **25**, as the wavefunction changes, at the same level. The S_1 state of both thiones has $n\pi^*$ character and is in the visible region. For **24** S_2 and S_3 are $\pi\pi^*$ and $n\pi^*$ states, respectively, while for **25** the reverse order has been obtained. S_2 and S_3 are in the range from ~ 3.5 to 5.2 eV, again at the highest level. It is the first time that the excited states of the title molecules are studied. The computed results agree with the experimental onsets of photoreactions of thiones **24** and **25** found by Reva *et al.* (*Phys. Chem. Chem. Phys.* **2015**, *17*, 4888).

Introduction

Cyclohexa-2,4-diene-1-thione (**24**; Figure 1) has been identified in a ground state isomerization reaction of thiophenol, studied at the MP2 and QCISD(T) levels by Al-Muhtaseb *et al.*^[1] Those authors obtained a very large barrier of ~ 63 kcal/mol for the thiophenol \rightarrow **24** thiol-thione H-transfer reaction. Although formation of the analogous cyclohexa-2,5-diene-1-thione (**25**; see Figure 1) has also been studied, the authors did not find a direct pathway for formation of **25** from thiophenol.^[1]

Reva *et al.*^[2] have isolated thiophenol in cryogenic argon matrices and observed the reversible photochemical thiophenol \leftrightarrow **24** and **24** \leftrightarrow **25** reactions. This was the first experimental observation of thione isomers **24** and **25**. According to the authors, the direct thiophenol \leftrightarrow **25** photoisomerization reaction could not be discarded nor confirmed.^[2]

In the present work the first three excited singlet states of **24** and **25** have been studied at the MR-CIS and MR-CISD levels, with inclusion of extensivity corrections (hereafter named +Q). Basis set effects were also taken into account. The results obtained for the two investigated systems were then used to address the excited states reached in the photochemical experiments performed by Reva *et al.*^[2] This is the first time that the excited states of thiones **24** and **25** are studied.

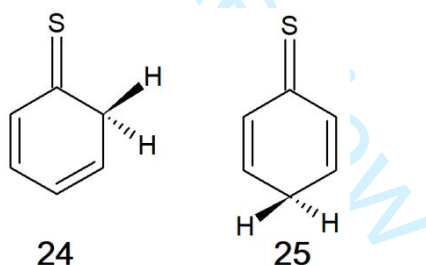


Figure 1. Thione isomers of thiophenol: cyclohexa-2,4-diene-1-thione (**24**, reads: “two-four”) and cyclohexa-2,5-diene-1-thione (**25**, reads “two-five”).

Computational Methods

The optimized structures of molecules **24** and **25** have been taken from ref.^[2] (B3LYP/aug-cc-pVTZ data). Frequency calculations have also been performed in ref.^[2], confirming that the obtained structures correspond to minima. Molecules **24** and **25** have C_s and C_{2v} symmetry, respectively.

In the present study, the active space used for thiones **24** and **25** at the CASSCF level (state average calculations) consists of 12 electrons in 11 orbitals. Two A' and two A'' states have been averaged at the CASSCF level for **24**, while for **25** one state for each one of the four symmetries (A₁, B₁, B₂ and A₂) has been averaged (in both cases with the same weights). For both systems these are the four lowest states at the CASSCF level. Due to the equivalence between the two C_{sp3}-H bonds of **24** and **25**, the σ orbitals in these molecules are equally localized on these bonds. Two pairs of active σ orbitals, the $\sigma_{C-H}/\sigma^*_{C-H}$ and $\sigma_{CS}/\sigma^*_{CS}$ pairs, have been included for both **24** and **25**. The C atom of the former pair is the sp³ C atom, for both molecules (see *Figure 1*).

For **25**, three of the six active π orbitals are named $\pi_{CS}+\pi_{ring}$ ($\equiv \pi_1$), n_π ($\equiv \pi_3$, an essentially non-bonding S orbital) and $\pi_{C=C}$ (that is, mainly localized on the C=C bonds, named π_2). The other non-bonding S orbital, perpendicular to the previous one, is simply named n , and the three anti-bonding π orbitals are named $\pi^*_{CS}+\pi^*_{ring}$ ($\equiv \pi_1^*$), $\pi^*_{C=C}$ ($\equiv \pi_2^*$) and π^*_{ring} ($\equiv \pi_3^*$).

For **24**, a non-bonding S orbital is again named n (as for **25**). The three bonding active π orbitals are named π_I , π_{CS} ($\equiv \pi_2$) and $\pi_S+\pi_{C=C}$ ($\equiv \pi_3$), while the anti-bonding orbitals are named $\pi^*_{ring}+\pi^*_{CS}$ ($\equiv \pi_1^*$), $\pi^*_{ring}+\pi^*_{CS}$ ($\equiv \pi_2^*$) and $\pi^*_{C=C}$ ($\equiv \pi_3^*$).

The subscripts of the orbitals (such as CS , $C=C$, etc.) refer to their localization. Additional details can be found in the supporting information.

The $\sigma_{CH}/\sigma^*_{CH}$ pairs of **24** and **25** have been included in the active space (for most of the wavefunctions here used) as this study is the first step towards a description (on the same grounds) of photoinduced hydrogen migration pathways associated with the thiophenol→**24**, thiophenol→**25** and **24**→**25** reactions. Besides, the above mentioned active space was constructed considering also the following two reasons: (i) as some preliminary calculations at the CASSCF level performed for thiophenol showed that the $\sigma_{CS}/\sigma^*_{CS}$ pair should be included in the active space, due to its admixture with the $\sigma_{SH}/\sigma^*_{SH}$ pair, the former pair has also been included in the active spaces of **24** and **25** (for most of the wavefunctions here used), due to the thiophenol→**24** and thiophenol→**25** reactions,^[2] which we intend to study; (ii) the highest level results for thiophenol (at the CASPT2 level, discussed later and compared to the results here obtained) include the eleven orbitals which transform into the eleven orbitals here used for **24** and **25**, along the thiophenol→**24** and thiophenol→**25** reaction pathways (as will be discussed elsewhere).

Five types of wavefunctions have been used in this work, named $w1$, $w1'$, $w2$, $w3$ and $w4$. $w1$ and $w1'$ are MR-CIS wavefunctions, while the remaining are MR-CISD wavefunctions. $w1$, $w1'$ and $w4$ are used for both systems. $w2$ is only used for **25**. For $w2$ the CAS space has been reduced, transferring strongly and weakly occupied orbitals to the doubly occupied (DOCC) and auxiliary (AUX) spaces, respectively, as discussed below. $w1'$ is derived from $w2$ simply reducing the internal \rightarrow external excitation level from singles and doubles to singles only (see Table 1). For $w3$ the CAS orbitals are split into reduced active space (RAS) and auxiliary (AUX) orbitals. It was not possible to use $w3$ for **25**, as in this case single occupied \rightarrow anti-bonding excitations are not enough to generate the correct number of guess vectors for each irreducible representation. In the case of $w4$ the four σ orbitals have been removed from the CAS (at both CASSCF and MR-CI levels) and the n and π_1 orbitals ($2a''/9b_2$ and $3a''/3b_1$, respectively, see the supporting information) have been transferred to the RAS space, and only single RAS \rightarrow CAS excitations are allowed while generating the reference configuration state functions (CSFs), yielding a set of reference CSFs based on a CAS(4,5) + single RAS \rightarrow CAS excitations. Additional details concerning how these four wavefunctions are formed are given in Table 1.

$w2$ is the largest MR-CISD wavefunction here used (see Table 1) and has only been employed for **25**, due to its higher (C_{2v}) symmetry (see Figure 1), but at the expense of a reduced number of active orbitals. This reduction consists of transferring former active orbitals, namely, two bonding (σ_{CS} and σ_{CH}) and three anti-bonding orbitals (σ_{CS}^* , σ_{CH}^* and π_{ring}^* , see supporting information) to the DOCC and AUX spaces, respectively, at the MR-CISD level.

The criteria chosen for these two sets of $w2$ were: the active orbitals whose occupation numbers (nocc) are (at the CASSCF level) larger than 1.97 have been transferred to the DOCC space, while those with $nocc < 0.1$ have been transferred to the AUX space, and only single CAS \rightarrow AUX excitations are allowed (yielding a set of reference CSFs based on a CAS(8,6) + single CAS \rightarrow AUX excitations, see Table 1). One can check the importance of double internal \rightarrow external excitations through a comparison between the results obtained from $w1'$ and $w2$. On the other hand, a comparison between $w1$ and $w1'$ allows checking the effect of the reference wave function on the relative accuracy of the MR-CIS wavefunctions.

Table 1. Wavefunctions used in this work, at the MR-CI level.

Wavefunction	excitation levels used to generate the reference CSFs ^a	Internal → external ^b excitation level/final MR-CI wavefunction
$w1$	CAS(12,11)	singles/MR-CIS
$w1'$	CAS(8,6) + single CAS → AUX excitations	singles/MR-CIS
$w2$	CAS(8,6) + single CAS → AUX excitations	singles and doubles/MR-CISD
$w3^c$	single occ → anti-bonding excitations	singles and doubles/MR-CISD
$w4$	CAS(4,5) + single RAS → CAS excitations	singles and doubles/MR-CISD

^aConfiguration State Functions; ^bInternal corresponds to the set of doubly occupied + active + AUX orbitals, while external corresponds to the set of orbitals which are unoccupied (virtual) in the reference CSFs; ^cFor $w3$ occ comprises the subset of six orbitals (active at the CASSCF level) with the highest occupation numbers, while the anti-bonding subset comprises the five active orbitals with the smallest occupation numbers. For additional details concerning these orbitals see text and supporting information.

Due to the size of the system and to the basis sets used, multi-reference configuration interaction calculations with single and double excitations (MR-CISD) are only feasible for **24** with a large reduction of the number of reference CSFs, at least for uncontracted MR-CI wavefunctions (as discussed later). Such reduction has been applied to yield the wavefunctions $w3$ and $w4$ (see Table 1). The first one has been devised with the purpose to see what is the net effect of reducing the internal excitation level (in other words, splitting the CAS into RAS + AUX orbitals) but at the same time increasing the internal → external excitation level, yielding an MR-CISD wavefunction. $w3$ has a similar size to that of $w1$. Again, due to the size of the system, an internal excitation level larger than one (between the occ and the anti-bonding subsets described in Table 1), combined with single and double internal → external excitations (yielding a MR-CISD wavefunction), is computationally prohibitive for **24**. However, the relatively small number of active orbitals used in $w4$ allows all excitations compatible with a CAS(4,5). Besides, as explained before, additional reference CSFs are also generated through RAS → CAS excitations (see Table 1). $w4$ corresponds to the largest CI expansion used for **24**.

Once the reference CSFs were formed, they were used to generate the excited CSF through single excitations from all internal into all external orbitals, at the MR-CIS level (for $w1$ and $w1'$, see Table 1), and through single and double internal → external excitations at the MR-CISD level (for $w2$, $w3$ and $w4$, see Table 1). The final CSF space is formed by the reference along with the excited CSFs.

There are two subsets of low-lying orbitals at the ground state geometries, the frozen core (FC) and the doubly occupied valence orbitals, at the MR-CIS/MR-CISD levels. The FC subset comprises the K (for the C atom) and K + L (for the S atom) shells. Such choice for the FC is based on the essentially correct description of the excited states of other systems containing another third row atom, Cl, at the MR-CISD level.^[3-10] The difference between doubly occupied and FC orbitals is that, while the former set remains doubly occupied only in the reference CSFs, the latter is kept as so in the reference as well as in the excited CSF space. The multireference extension of the Davidson correction (+Q) has been used to take the size-extensivity error into account.^[11-13] Rigorously speaking, the Davidson correction should only be used for CISD/MR-CISD wavefunctions, not for CIS/MR-CIS wavefunctions.^[13] According to eqs. (42) and (43) from ref. ^[13] it is clear that the stabilization due to the Davidson correction is always larger for an MR-CISD wavefunction, as compared to that for an MR-CIS wavefunction formed from the same set of reference CSFs. This is due to (i) the sum of the weights of the reference CSFs is always smaller in the MR-CISD than in the MR-CIS wavefunction; (ii) the final MR-CISD energy is always smaller than the final MR-CIS energy. Thus, as the final MR-CISD energy is always smaller than the final MR-CIS energy, the Davidson corrected MR-CISD energy is always smaller than the Davidson corrected MR-CIS energy. However, error cancellation effects can lead to similar Davidson corrections for the excitation energies computed with MR-CIS and MR-CISD wavefunctions (which is the case for the $w2$ and $w1'$ calculations performed for **25**, as discussed later). As such error cancellation effects are not guaranteed, one should be cautious while using the Davidson correction formula for MR-CIS wavefunctions.

The interactive space restriction^[14] has been used for $w2$ and $w4$ (see Table 1). All CASSCF, MR-CISD, and MR-CISD+Q calculations have been performed with the COLUMBUS program system.^[15-18] The atomic orbitals (AO) integrals used by COLUMBUS have been computed with the DALTON program.^[19] The aug-cc-pVTZ and the mixed aug-cc-pVDZ(C,H)/aug-cc-pVTZ(S) basis sets have been used in this study.^[20-22]

Results and discussion

Basis set effect

The basis set effect has been taken into account at the CASSCF level, for both systems (see Table 2), and at the $w1$ and $w4$ levels for **25** (see Table 3). As it can be seen from Tables 2 and 3, the ΔE values obtained with both basis sets differ by at most 0.03 eV. Besides, the

main configurations obtained for all four states do not change with the basis set, and the differences between their weights are virtually negligible, at CASSCF, $w1$ and $w4$ levels. Besides, the differences between the f values obtained with the two basis sets are small, at the $w1$ and $w4$ levels (see Table 3). Therefore, the results shown in Tables 2 and 3 give us confidence about the reliability of the aug-cc-pVDZ(C,H)/aug-cc-pVTZ(S) basis set towards the computationally much more demanding aug-cc-pVTZ(C,H,S) basis set.

Table 2. ΔE values (in eV) and configuration weights computed at the CASSCF level with the aug-cc-pVDZ(C,H)/aug-cc-pVTZ(S) basis set, for **24** and **25** thione isomers.

24			25		
State	ΔE	Configurations ^{a,b}	State	ΔE	Configurations ^{a,b}
1 ¹ A'	0.00	0.60gs + 0.25 $\pi_3\pi_1^*$	1 ¹ A ₁	0.00	0.75gs + 0.10 $n_\pi\pi_1^*$
1 ¹ A''	2.09 (2.07) ^c	0.80 $n\pi_1^*$	1 ¹ A ₂	2.18 (2.16) ^c	0.83 $n\pi_1^*$
2 ¹ A'	4.50 (4.49) ^c	0.21 $\pi_2\pi_1^*$ + 0.19 $\pi_3\pi_1^*$ + 0.15 $\pi_3^0\pi_1^{*2}$ + 0.12 $\pi_3\pi_2^*$	1 ¹ B ₁	4.98 (4.95) ^c	0.45 $n\pi_2^*$ + 0.29 $n^1\pi_2^1\pi_1^{*2}$
2 ¹ A''	4.55 (4.53) ^c	0.44 $n\pi_2^*$ + 0.23 $n^1\pi_3^1\pi_1^{*2}$ + 0.12 $n^1\pi_2^1\pi_1^{*2}$	1 ¹ B ₂	5.36 (5.35) ^c	0.28 $n_\pi\pi_2^*$ + 0.27 $\pi_2^1n_\pi^1\pi_1^{*2}$ + 0.19 $\pi_2\pi_1^*$

^ags stands for the ground state configuration; only configurations with weights larger than 0.1 are shown; ^bConfigurations a^0b^2 and $a^1b^1c^2$ correspond to the $a \rightarrow b$ and $(a,b) \rightarrow c$ double excitations, respectively, and the remaining configurations correspond to single excitations; ^cResults obtained with the aug-cc-pVTZ(C,H,S) basis set. The weights obtained with both basis sets differ by at most 0.01.

Vertically excited states of 24 and 25

ΔE values, configuration weights and oscillator strengths (f) computed with $w1$, $w2$, $w1'$ and $w4$ for **25** are shown in Table 3. As it can be seen through comparison between Tables 2 and 3, inclusion of dynamic electron correlation (at both MR-CIS and MR-CISD levels) changes the ΔE values by at most 0.41 eV. A decrease in the ΔE values is obtained upon inclusion of extensivity correction, but the effect is smaller than that of the dynamic electron correlation, leading to a maximum change of 0.19 eV. The nature of all studied states is the same, at the CASSCF and MR-CI levels (compare Tables 2 and 3). It is important to point out the non-negligible contribution of configurations formed by double excitations to the π_1^* orbital, in the 1¹B₁ and 1¹B₂ states, although these weights decrease upon inclusion of dynamic electron correlation (compare Tables 2 and 3).

1
2
3 An important difference between the results obtained for thione isomers **24** and **25** and
4 those obtained for the thiol isomer (thiophenol) is the absence of configurations formed by
5 excitations to the σ^* orbital, a feature observed for the S_2 state of thiophenol.^[23-27] However,
6 such difference is expected, as in thiophenol this orbital is localized on a considerably weaker
7 (S–H) bond.
8
9

10
11
12 Using the CASPT2/aug-cc-pVTZ results for thiophenol as reference^[23] (4.3, 4.5 and 5.1
13 eV for the S_1 , S_2 and S_3 states, respectively), one can see a decrease in the excitation energies
14 (as one goes from thiophenol to **25**), with the largest effect obtained for the first excited state,
15 followed by the second excited state. Compared to the highest level $w2(+Q)$ results (as
16 discussed later), the decrease for S_1 is as large as ~ 2.1 eV, while for S_2 one has an increase of
17 only ~ 0.3 eV, at the same level. For S_3 the changes are almost negligible, at both $w2(+Q)$ and
18 $w4(+Q)$ levels. For $w1$ and $w1'$ decreases of ~ 0.3 eV are obtained (see Table 3). It is
19 important to stress that one should be cautious while comparing results obtained with
20 different methods, for different molecules, as part of the difference is likely to be due to the
21 methods. Nevertheless, as a much larger effect has been observed for S_1 , it is very likely that
22 at least in this case the obtained trend is correct.
23
24
25
26
27
28
29
30
31

32 It is interesting to point out the change of nature of S_1 of the thione isomer **25** as
33 compared to the thiol form of thiophenol. Although there is some contribution of the n orbital
34 (perpendicular to the π system of the ring) to the σ_{SH} and σ_{SC} orbitals of thiophenol,^[24]
35 configurations containing excitations from these orbitals are absent in the lowest four excited
36 states of thiophenol.^[23-27] On the other hand, in **25** (and also in **24**, as discussed later) the n
37 orbital is very well localized (as shown in the supporting information). While in thiophenol S_1
38 is a $\pi\pi^*$ state, in **25** it is an $n\pi^*$ state (see Table 3). S_2 is also an $n\pi^*$ state, and S_3 is a $\pi\pi^*$ state
39 (see Table 3). Thus, only the nature of S_3 is the same both in thiophenol^[23] and in the thione
40 isomer **25**.
41
42
43
44
45
46
47

48 The first excited state of **25** (1^1A_2) is in the visible region (with $\Delta E = 2.15$ or 2.36 eV, at
49 the $w2(+Q)$ and $w4(+Q)$ levels, respectively), but the $1^1A_1 \rightarrow 1^1A_2$ transition is dipole
50 forbidden, by symmetry. However, the experimental threshold required for photochemical
51 transformations of **25**, $\lambda < 332$ nm (3.73 eV), is consistent with a transition within the first
52 band (see Table 3). Therefore, some intensity gain is expected to be taking place around 3.73
53 eV, due to vibronic and/or spin-orbit coupling mechanisms. Besides, one cannot rule out some
54 intensity borrowing from the nearby $S_0 \rightarrow S_2$ transition.
55
56
57
58
59
60

Table 3. ΔE values (in eV), configuration weights and oscillator strengths (f) computed for **25**, at the $w1, w2, w1'$ and $w4$ levels (see Table 1), with the aug-cc-pVDZ(C,H)/aug-cc-pVTZ(S) basis set. Multireference extension of the size-extensivity Davidson correction is indicated by (+Q).

Wavefunction $w1$				
States	ΔE	$\Delta E (+Q)$	$f(\times 10^3)$	configurations ^{a,b}
1^1A_1	0.00	0.00	--	0.74gs
1^1A_2	2.04 (2.03) ^c	2.00 (1.99) ^c	-- ^d	$0.80n\pi_1^*$
1^1B_1	4.65 (4.62) ^c	4.50 (4.47) ^c	0.557(0.524) ^c	$0.60n\pi_2^* + 0.14n^1\pi_2^1\pi_1^{*2}$
1^1B_2	4.98 (4.97) ^c	4.84 (4.82) ^c	20.062 (19.688) ^c	$0.35n\pi_2\pi_1^* + 0.22n\pi_2\pi_1^* + 0.21n\pi_2^1\pi_1^{*2}$
Wavefunction $w2$				
States	ΔE	$\Delta E (+Q)$	$f(\times 10^3)$	configurations ^{a,b}
1^1A_1	0.00	0.00	--	0.65gs
1^1A_2	2.12	2.15	-- ^d	$0.72n\pi_1^*$
1^1B_1	4.90	4.82	0.098	$0.46n\pi_2^* + 0.20n^1\pi_2^1\pi_1^{*2}$
1^1B_2	5.17	5.07	15.326	$0.25n\pi_2\pi_1^* + 0.22n\pi_2\pi_1^* + 0.21n\pi_2^1\pi_1^{*2}$
Wavefunction $w1'$				
States	ΔE	$\Delta E (+Q)$	$f(\times 10^3)$	configurations ^{a,b}
1^1A_1	0.00	0.00	--	0.74gs
1^1A_2	2.08	2.08	-- ^d	$0.80n\pi_1^*$
1^1B_1	4.76	4.63	0.649	$0.60n\pi_2^* + 0.14n^1\pi_2^1\pi_1^{*2}$
1^1B_2	4.95	4.79	25.929	$0.34n\pi_2\pi_1^* + 0.22n\pi_2\pi_1^* + 0.21n\pi_2^1\pi_1^{*2}$
Wavefunction $w4$				
States	ΔE	$\Delta E (+Q)$	$f(\times 10^3)$	configurations ^{a,b}
1^1A_1	0.00	0.00	--	0.65gs
1^1A_2	2.47 (2.45) ^c	2.36 (2.36) ^c	-- ^d	$0.74n\pi_1^*$
1^1B_1	5.25 (5.23) ^c	5.06 (5.05) ^c	0.115 (0.092) ^c	$0.51n\pi_2^* + 0.19n^1\pi_2^1\pi_1^{*2}$
1^1B_2	5.18 (5.17) ^c	5.07 (5.06) ^c	16.395 (15.180) ^c	$0.26n\pi_2\pi_1^* + 0.22n\pi_2^1\pi_1^{*2} + 0.21n\pi_2\pi_1^*$

^ags stands for the ground state configuration; only configurations with weights larger than 0.1 are shown. The weights obtained with both basis sets (for $w1$) differ by at most 0.01; ^bConfigurations $a^1b^1c^2$ correspond to the (a,b) \rightarrow c double excitations, while the remaining configurations correspond to single excitations; ^cResults obtained with the aug-cc-pVTZ(C,H,S) basis set; ^dForbidden by symmetry. For $w1$ and $w1'$ the total MR-CIS/MR-CIS+Q energies are (in au) -628.524468/-628.542458 and -628.470817/-628.487837, respectively; For $w2$ and $w4$ the total MR-CISD/MR-CISD+Q energies are -629.081146/-629.2309174 and -629.079709/-629.229106, respectively.

1
2
3 Due to the judicious choice of the CASSCF active orbitals to be transferred to the
4 DOCC and AUX spaces while forming the reference set of CSFs for w_2 (see Table 1 and the
5 previous discussion concerning the criteria used for this transfer), it is expected that w_2
6 already recovers a large fraction of the electron correlation of an MR-CISD wavefunction
7 formed from a set of CAS(12,11) reference CSFs. Consequently, the results obtained with w_2
8 can be considered the most reliable ones for **25**. As already mentioned, w_2 is the largest MR-
9 CI wavefunction here employed, achieving 3.6×10^8 CSFs.

10
11 From what has been said one can test the reliability of $w_{I'}$ for **25** comparing its results
12 with those obtained from w_2 . Such comparison allows addressing the importance of the
13 double internal→external excitations (see Table 1). As it can be seen from Table 3, the
14 computed excitation energies are close, with a maximum difference of 0.28 eV, obtained for
15 1^1B_2 including extensivity corrections. The main configurations are maintained, for $w_{I'}$ and
16 w_2 , and the largest change obtained for the configuration weights is 0.14 (for 1^1B_1), a value
17 which can be considered relatively small. On the other hand, the effect on the f values, due to
18 the change from $w_{I'}$ to w_2 , is significant, with reductions down to ~15 and 59% for 1^1B_1 and
19 1^1B_2 , respectively (see Table 3). Despite such reduction, the $S_0 \rightarrow S_3$ transition remains the
20 most intense one for both wavefunctions. Therefore, $w_{I'}$ can be considered a relatively good
21 approximation to w_2 (a computationally much more demanding wavefunction). Besides, due
22 to the error cancellation effects mentioned previously, the size-extensivity correction in the
23 ΔE values computed with $w_{I'}$ and w_2 are similar (see Table 3).

24
25 As can be seen from Table 3 the effect associated with the change from w_I to $w_{I'}$ is
26 smaller than that between w_2 and $w_{I'}$, for the ΔE and f values. ΔE values change by at most
27 0.13 eV, and the f values increase ~ 16 and 29 % for the $S_0 \rightarrow S_2$ and $S_0 \rightarrow S_3$ transitions,
28 respectively, while changing the wavefunction from w_I to $w_{I'}$. The main configurations
29 remain the same as well as their weights virtually don't change upon the change from w_I to
30 $w_{I'}$ (see Table 3).

31
32 Through a comparison between w_2 and w_4 one can verify how good the latter as an
33 approximation to the former is. Without extensivity correction the largest difference between
34 the ΔE values computed with w_2 and w_4 is 0.35 eV. Upon inclusion of extensivity correction
35 one has slightly smaller differences, of at most 0.24 eV. Interestingly, either with or without
36 extensivity correction the difference between the ΔE values of S_3 , obtained from w_2 or w_4 , is
37 virtually negligible (see Table 3). As the wavefunction changes from w_2 to w_4 the f values
38 increase only ~ 15 and 7 % for the $S_0 \rightarrow S_2$ and $S_0 \rightarrow S_3$ transitions, respectively. Again, the

1
2
3 main configurations are maintained and their weights change by at most 0.05, from w_2 to w_4
4 (see Table 3). Thus, w_4 can be considered a good approximation to w_2 , especially if
5 extensivity correction is included.
6
7

8
9 ΔE values, configuration weights and oscillator strengths (f) computed with w_1 , w_1' , w_3
10 and w_4 for **24** are shown in Table 4. It is clear that the effect of dynamic electron correlation
11 is considerably larger for the ΔE values of **24** than for those of **25** (especially for S_2 and S_3)
12 and the effect for the latter is slightly dependent on the state (compare Table 2 with Tables 3
13 and 4). On the other hand, for **24** the effect of dynamic electron correlation is highly
14 dependent on the state and on the wavefunction. For instance, as for the $2^1A'$ (S_2) state
15 computed with w_1 a reduction of 0.68 eV is obtained, for the same state calculated with w_3
16 and w_4 one has reductions of only 0.24 and 0.19 eV, respectively, upon inclusion of dynamic
17 electron correlation. However, in the case of the fourth state ($2^1A''$) a much larger change is
18 obtained for w_3 , as compared to that obtained for w_1 (0.92 versus 0.23 eV). In contrast, for
19 w_4 one has a slight increase of 0.28 eV (compare the CASSCF and MR-CI results from
20 Tables 2 and 4, respectively).
21
22
23
24
25
26
27
28

29
30 Albeit the nature of the excited states (that is, $n\pi^*$ or $\pi\pi^*$) of **24** does not change upon
31 inclusion of dynamic electron correlation, the multiconfigurational character of S_2 and S_3
32 decreases significantly as dynamic electron correlation is included (compare Tables 2 and 4).
33
34

35
36 In the case of the S_1 state of **24** and **25** the effect of extensivity correction is similar and
37 small, changing the ΔE values by at most 0.11 and 0.12 eV, for **25** and **24**, respectively, both
38 obtained with w_4 . For the S_2 and S_3 states of **24** the effect is significantly larger, decreasing
39 the ΔE values of S_2 and S_3 by at most 0.32 and 0.22 eV, respectively (see Table 4).
40
41
42

43 It is important to point out that, even considering only single internal \rightarrow external
44 excitations from the reference CSFs generated at the CAS(12,11) level (as in w_1 , see Table 1),
45 for **24** the final number of CSFs is already very large, $\sim 2.1 \times 10^8$ CSFs, due to the system
46 size, number of active orbitals and basis set. Therefore, if one includes single and double
47 excitations, the calculation becomes computationally prohibitive, at least for an uncontracted
48 multi-reference CI wavefunction, which is the type of MR-CI wavefunctions used in this
49 work.^[28] The same can be said even if one uses the same type of active space reduction based
50 on the CASSCF occupation numbers, as it has been done for the wavefunction w_2 of **25**.
51
52
53
54
55
56
57
58
59
60

Table 4. ΔE values (in eV), configuration weights and oscillator strengths (f) computed for **24**, at the $w1$, $w1'$, $w3$ and $w4$ levels (see Table 1), with the aug-cc-pVDZ(C,H)/aug-cc-pVTZ(S) basis set. Multireference extension of the size-extensivity Davidson correction is indicated by (+Q).

Wavefunction $w1$				
States	ΔE	ΔE (+Q)	$f(\times 10^3)$	configurations ^{a,b}
1 ¹ A'	0.00	0.00	--	0.62gs + 0.19 $\pi_3\pi_1^*$
1 ¹ A''	1.92	1.88	0.052	0.79n π_1^*
2 ¹ A'	3.82	3.54	248.8	0.54 $\pi_3\pi_1^*$ + 0.16gs
2 ¹ A''	4.32	4.22	0.061	0.52n π_2^* + 0.18n ¹ $\pi_3^1\pi_1^{*2}$
Wavefunction $w1'$				
States	ΔE	ΔE (+Q)	$f(\times 10^3)$	configurations ^{a,b}
1 ¹ A'	0.00	0.00	--	0.63gs + 0.19 $\pi_3\pi_1^*$
1 ¹ A''	1.95	1.96	0.052	0.81n π_1^*
2 ¹ A'	3.88	3.56	293.0	0.57 $\pi_3\pi_1^*$ + 0.18gs
2 ¹ A''	4.38	4.31	0.073	0.51n π_2^* + 0.20n ¹ $\pi_3^1\pi_1^{*2}$
Wavefunction $w3$				
States	ΔE	ΔE (+Q)	$f(\times 10^3)$	configurations ^{a,b}
1 ¹ A'	0.00	0.00	--	0.61gs + 0.16 $\pi_3\pi_1^*$
1 ¹ A''	2.27	2.36	0.053	0.77n π_1^*
2 ¹ A'	4.26	4.06	317.1	0.53 $\pi_3\pi_1^*$ + 0.13gs
2 ¹ A''	5.47	5.25	0.033	0.76n π_2^*
Wavefunction $w4$				
States	ΔE	ΔE (+Q)	$f(\times 10^3)$	configurations ^{a,b}
1 ¹ A'	0.00	0.00	--	0.56gs + 0.16 $\pi_3\pi_1^*$
1 ¹ A''	2.31	2.19	0.041	0.73n π_1^*
2 ¹ A'	4.31	4.09	179.8	0.32 $\pi_3\pi_1^*$ + 0.13 $\pi_2\pi_1^*$
2 ¹ A''	4.83	4.62	0.001	0.46n π_2^* + 0.19n ¹ $\pi_3^1\pi_1^{*2}$

^ags stands for the ground state configuration; only configurations with weights larger than 0.1 are shown; ^bConfigurations a¹b¹c² correspond to the (a,b)→c double excitations, while the remaining configurations correspond to single excitations. For $w1$, $w1'$, $w3$ and $w4$ the total MR-CI/MR-CI+Q energies are (in au) -628.521163/-628.539777, -628.466399/-628.484396, -629.050072/-629.212969 and -629.073981/-629.225881, respectively.

1
2
3 One very important point is what type of wavefunction recovers a larger fraction of the
4 electron correlation provided by a complete MR-CISD wavefunction, that is, an MR-CISD
5 wavefunction based on a set of CAS(12,11) reference CSFs. As already mentioned, such type
6 of calculation is not affordable, at least for an uncontracted wavefunction. However, one has
7 two affordable options: (i) only single internal \rightarrow external excitations, yielding an MR-CIS
8 wavefunction ($w1$, see Table 1); (ii) an MR-CISD wavefunction based on reference CSFs
9 generated through limited excitations among the internal orbitals (from the occ to the anti-
10 bonding orbitals described in Table 1), as in the case of $w3$ (for which only single occ \rightarrow anti-
11 bonding excitations have been applied, see Table 1). Though the answer concerning which
12 type of wavefunction, $w1$ or $w3$, recovers a larger fraction of the electron correlation provided
13 by a complete MR-CISD wavefunction could not be obtained, one can compare the effect due
14 to the change from $w1$ to $w3$ on the properties here studied for **24** (see Table 4). As case (ii)
15 calculations based on higher than single excitations are not affordable, one could not study the
16 effect of the excitation level (within the internal orbitals given in Table 1) on the final
17 properties. Instead, one can study the effect of removing the σ orbitals and, at the same time,
18 increasing the excitation level within the active orbitals, through comparison between $w3$ and
19 $w4$ (see Table 1).

20
21
22 As can be seen from Table 4, there are relatively large differences between the ΔE
23 results obtained with $w1$ and with the MR-CISD wavefunctions ($w3$ and $w4$, see Table 1),
24 varying from 0.31 to 1.15 eV, and the maximum difference has been obtained for S_3 ($2^1A''$)
25 either with or without extensivity corrections. On the other hand, the differences between the
26 ΔE values obtained with $w3$ and $w4$, for S_1 ($1^1A''$) and S_2 ($2^1A'$), are almost negligible
27 (varying from 0.03 to 0.17 eV, see Table 4). For S_3 the differences between the $w3$ and $w4$
28 results are much larger (with values of 0.63 and 0.64 eV, with and without extensivity
29 corrections, respectively, see Table 4). Therefore, it is clear that the ΔE values obtained for S_3
30 shows by far the largest average variation among the wavefunctions (see Table 4), which can
31 be taken as an evidence of the greater difficulty in describing this state.

32
33
34 Similarly to what has been obtained for **25**, the effect due to the change from $w1$ to $w1'$
35 is small, leading to changes of at most 0.09 and 0.06 eV in the ΔE values, with and without
36 extensivity corrections, respectively. The f value of the $S_0 \rightarrow S_1$ transition practically does not
37 change, while those of the $S_0 \rightarrow S_2$ and $S_0 \rightarrow S_3$ transitions increase only ~ 18 and $\sim 20\%$,
38 respectively (see Table 4).

1
2
3 Based on the similarity between **24** and **25** and on the comparison between the results
4 for **25**, obtained from $w2$ and $w4$, it is expected that $w4$ is a good approximation to $w2$ also for
5 **24**, especially if extensivity correction is included, as aforementioned. Thus, $w4$ is not only
6 the largest wavefunction used for **24**, but can also be considered the most reliable one.
7
8 Consequently, the discrepancies between $w1/w1'$ and $w4$ are likely to be due to the
9 unreliability of the former.

10
11
12
13
14 Despite the relatively large differences between the ΔE values (especially for S_3 , see
15 Table 4), the nature of the states does not change with the wavefunction, even though there
16 are some significant variations of the multiconfigurational character of S_2 and S_3 (see Table
17 4). Nevertheless, although the multiconfigurational character of S_2 is larger for $w4$, the weight
18 of the ground state configuration is virtually negligible in this case, differently of what
19 happens for $w1$, $w1'$ and $w3$ (see Table 4). For all three wavefunctions there are significant
20 contributions of the $\pi_3\pi_1^*$ configuration in the ground state wavefunction. For the S_3 state one
21 has significant contributions of a double excitation ($n^1\pi_3^1\pi_1^{*2}$) only for $w1$ and $w4$ (see Table
22 4), which is expected, as the reference CSFs of $w3$ do not include this double excitation (cf.
23 Table 1).

24
25
26
27
28 For all three wavefunctions the most intense transition of **24** remains the same ($1^1A' \rightarrow$
29 $2^1A'$, $S_0 \rightarrow S_2$, see Table 4). Based on the results obtained for the f values of **25** (and again
30 based on the fact that **24** and **25** are similar), some decrease on the f values of **24** is to be
31 expected (due to the change from $w4$ to $w2$), if $w2$ was not computationally prohibitive for **24**.
32 However, it is not expected that the most intense transition changes. Such transition for **24**
33 ($1^1A' \rightarrow 2^1A'$) is approximately 11 times more intense than that of **25** ($1^1A_1 \rightarrow 1^1B_2$, compare
34 the $w4$ results in Tables 3 and 4). This information, along with their corresponding excitation
35 energies of 4.09 and 5.07 eV (obtained at the $w4(+Q)$ level for **24** and **25**, respectively, see
36 Tables 3 and 4), can be helpful if one wants to discriminate these two isomers through UV-
37 VIS absorption spectroscopy.

38
39
40
41
42 By comparison between the CASPT2/aug-cc-pVTZ results for thiophenol, used as
43 reference^[23] (4.3, 4.5 and 5.1 eV for the S_1 , S_2 and S_3 states, respectively), and those obtained
44 for **24**, one can see how the ΔE values change in the thiophenol vs. **24** pair. It is clear that the
45 effect is by far the largest for S_1 (as in the thiophenol vs. **25** pair). Comparing the CASPT2
46 results with the results obtained including extensivity corrections (+Q), the excitation energies
47 of S_1 decrease by ~ 2.1 to 2.4 eV, depending on the wavefunction (see Table 4). With
48
49
50
51
52
53
54
55
56
57
58
59
60

exception of S_3 at the $w3(+Q)$ level (where a slight increase of only 0.15 eV is obtained), the other $\Delta E(+Q)$ values of S_2 and S_3 decrease from 0.41 to 0.96 eV, depending on the state and on the level of theory used, again compared to the CASPT2 results (see Table 4).

The $\Delta E(+Q)$ values of S_1 (see Table 4), along with the computed f values (although very small), are in line with the observation from ref.^[2] that **24** is the only isomer which absorbs in the visible region. As discussed before, even if the first excited state of **25** is also in the visible region, its transition dipole moment vanishes by symmetry.

The experimental threshold for the photochemical transformations of **24** ($\lambda < 427$ nm = 2.90 eV) is consistent with excitation within the first band, associated with $1^1A''$ (an $n\pi^*$ state; see Table 4). While in thiophenol S_1 is a $\pi\pi^*$ state, in **24** it is an $n\pi^*$ state, followed by an $\pi\pi^*(S_2)$ and an $n\pi^*(S_3)$ state (see Table 4). Thus, the nature of all three excited states change as one goes from thiophenol^[23] to the thione isomer **24**. For **24** and **25** the most intense band is due to a transition to a $\pi\pi^*$ state, for all wavefunctions (see Tables 3 and 4).

Conclusions

The first four singlet states of thiones **24** and **25** have been studied using several types of uncontracted MR-CI wavefunctions, with the mixed aug-cc-PVDZ(C,H)/aug-cc-pVTZ(S) basis set. Excitation energies (ΔE), oscillator strengths (f) and nature of the excited states have been investigated. The basis set effect has also been taken into account. It is the first time that the excited states of **24** and **25** are studied.

The largest MR-CI calculation has been here performed for **25**, due to its C_{2v} symmetry, achieving $\sim 3.6 \times 10^8$ CSFs. The change from thiophenol to **25** largely decreases the excitation energy of S_1 (based on previous CASPT2/aug-cc-pVTZ^[23] and the $\Delta E(+Q)$ results, see Table 3). In the case of S_2 , the effect is opposite but much smaller, increasing its excitation energy by at most 0.56 eV (at the $-w4(+Q)$ level, see Table 3). In the case of S_3 the effect is almost negligible for the MR-CISD wavefunctions ($w2$ and $w4$, see Table 3).

Although S_1 of **25** (1^1A_2) is in the visible region (with $\Delta E(+Q)$ from ~ 2.0 to 2.4 eV, see Table 3), the $1^1A_1 \rightarrow 1^1A_2$ transition is dipole forbidden, by symmetry. The experimental threshold required for photochemical transformations of **25**, $\lambda < 332$ nm (3.73 eV^[2]) is, according to our results, consistent with a transition within the first band. Therefore, some

intensity gain is expected to be taking place around 3.73 eV, due to vibronic and/or spin-orbit coupling mechanisms. Intensity borrowing from the nearby band cannot be ruled out.

Only the nature of S_3 (a $\pi\pi^*$ state) is maintained as thiophenol changes to **25**, with both S_1 (also a $\pi\pi^*$ state) and S_2 (an $n_\pi\sigma^*$) excited states changing their nature to $n\pi^*$. On the other hand, for **24** the nature of the three first excited singlet states is $n\pi^*$, $\pi\pi^*$ and $n\pi^*$, respectively. Thus, the nature of S_1 to S_3 changes upon the thiophenol→**24** isomerization.

The ΔE values decrease largely with the thiophenol→**24** isomerization (again based on previous CASPT2/aug-cc-pVTZ^[23] and $\Delta E(+Q)$ results), especially for S_1 . The only exception is observed for S_3 with w_3 (see Table 4). The $\Delta E(+Q)$ values, along with the computed f values (although very small), are in line with the observation from ref.^[2] that **24** is the sole isomer absorbing in the visible region. The experimental threshold for the photochemical transformations of **24** ($\lambda < 427 \text{ nm} = 2.90 \text{ eV}$) is consistent with excitation within the first band, associated with the $1^1A''$ (an $n\pi^*$) state.

Despite the relatively large differences obtained for the f values computed with different wavefunctions, the $S_0 \rightarrow S_3$ transition of **25** remains the most intense for all wavefunctions studied for this molecule. The same holds for the $S_0 \rightarrow S_2$ transition of **24**.

Larger uncontracted MR-CI calculations still need to be performed (e.g., MR-CISD based on a set of CAS(12,11) reference CSFs), when they become computationally feasible, to see how the aforementioned results are affected. Alternatively, the effect of using more accurate extensivity corrections, as multi-reference average quadratic, MR-AQCC, might be evaluated in relation to alterations in the excited states' properties.^[29]

Acknowledgements

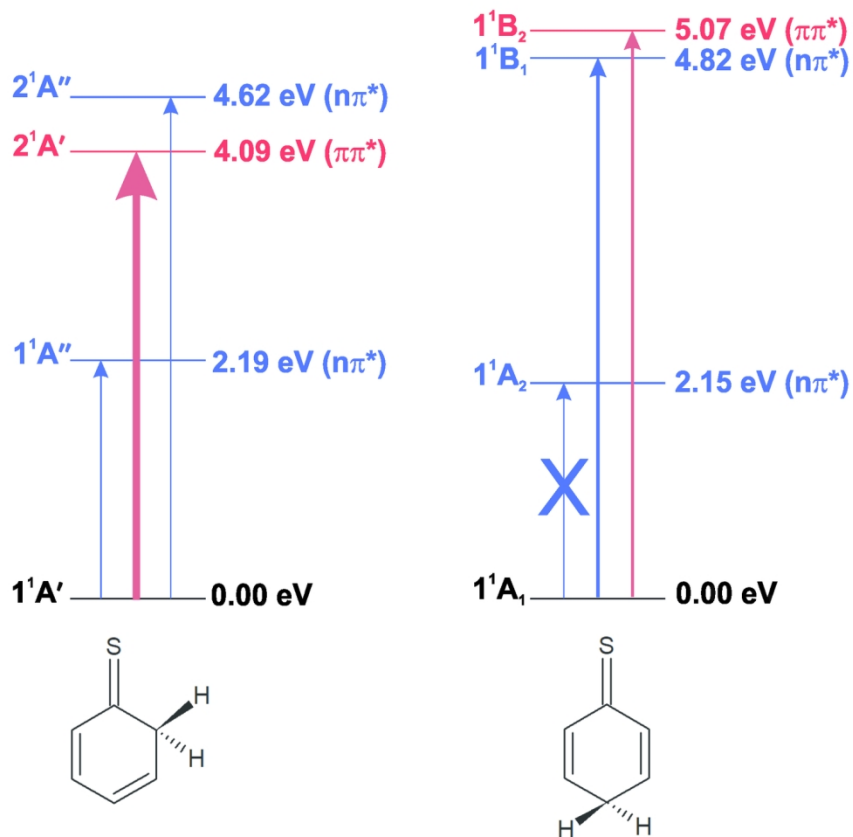
I. R. acknowledges the Portuguese Foundation for Science and Technology (FCT) for an *Investigador FCT* grant. R.F. and I. R. thank FCT for financial support to the Coimbra Chemistry Centre (CQC, Research Unit UI0313/QUI/2020) co-funded by FEDER/COMPETE 2020-EU. E.V. thanks the Brazilian agency CNPq (Grant Number 303884/2018-5 and 423112/2018-0) for support. The remaining authors are grateful to the Brazilian agencies CAPES and FINEP for financial support. They are also thankful to the CESUP/UFRGS supercomputing center for the computational facilities.

References

- [1] A. H. Al-Muhtaseb, M. Altarawneh, M. H. Almatarneh, *J Comput. Chem.* **2011**, *32*, 2708. <https://doi.org/10.1002/jcc.21852>.
- [2] I. Reva, M. J. Nowak, L. Lapinski, R. Fausto, *Phys. Chem. Chem. Phys.* **2015**, *17*, 4888. <https://doi.org/10.1039/C4CP04125A>.
- [3] G. P. Rodrigues, T. M. L. de Lima, R. B. de Andrade, E. Ventura, S. A. do Monte, M. Barbatti, *J. Phys. Chem. A* **2019**, *123*, 1953. <https://doi.org/10.1021/acs.jpca.8b12482>.
- [4] V. C. de Medeiros, R. B de Andrade, G. P. Rodrigues, G. F. Bauerfeldt, E. Ventura, M. Barbatti, S. A. do Monte, *J. Chem. Theory Comput.* **2018**, *14*, 4844. <https://doi.org/10.1021/acs.jctc.8b00457>.
- [5] V. C. de Medeiros, R. B de Andrade, E. F. V. Leitão, E. Ventura, G. F. Bauerfeldt, M. Barbatti, S. A. do Monte, *J. Am. Chem. Soc.* **2016**, *138*, 272. <https://doi.org/10.1021/jacs.5b10573>.
- [6] V. C. de Medeiros, S. A. do Monte, E. Ventura, *RSC Adv.* **2014**, *4*, 64085. <https://doi.org/10.1039/C4RA10567B>.
- [7] G. P. Rodrigues, E. Ventura, S. A. do Monte, M. Barbatti, *J. Phys. Chem. A* **2014**, *118*, 12041. <https://doi.org/10.1021/jp507681g>.
- [8] G. P. Rodrigues, J. R. Lucena Jr., E. Ventura, S. A. do Monte, I. Reva, R. Fausto, *J. Chem. Phys.* **2013**, *139*, 204302. <https://doi.org/10.1063/1.4832376>.
- [9] V. C. de Medeiros, E. Ventura, S. A. do Monte, *Chem. Phys. Lett.* **2012**, *546*, 30. <https://doi.org/10.1016/j.cplett.2012.07.037>.
- [10] J. R. Lucena Jr., E. Ventura, S. A. do Monte, R. C. M. U. Araújo, M. N. Ramos, *J. Chem. Phys.* **2007**, *127*, 164320. <https://doi.org/10.1063/1.2800020>.
- [11] S. R. Langhoff, E. R. Davidson, *Int. J. Quantum Chem.* **1974**, *8*, 61. <https://doi.org/10.1002/qua.560080106>.
- [12] P. J. Bruna, S. D. Peyerimhoff, R. J. Buenker, *Chem. Phys. Lett.* **1980**, *72*, 278. [https://doi.org/10.1016/0009-2614\(80\)80291-0](https://doi.org/10.1016/0009-2614(80)80291-0).
- [13] P. G. Szalay, T. Müller, G. Gidofalvi, H. Lischka, R. Shepard, *Chem. Rev.* **2012**, *112*, 108. <https://doi.org/10.1021/cr200137a>.
- [14] A. Bunge, *J. Chem. Phys.* **1970**, *53*, 20. <https://doi.org/10.1063/1.1673766>.
- [15] R. Shepard, I. Shavitt, R. M. Pitzer, D. C. Comeau, M. Pepper, H. Lischka, P. G. Szalay, R. Ahlrichs, F. B. Brown, J. Zhao, *Int. J. Quantum Chem.* **1988**, *34*, 149. <https://doi.org/10.1002/qua.560340819>.
- [16] H. Lischka, R. Shepard, I. Shavitt, R. M. Pitzer, M. Dallos, T. Müller, P. G. Szalay, F. B. Brown, R. Ahlrichs, H. J. Böhm, *et. al.* COLUMBUS, an Ab Initio Electronic Structure Program, Release 7.0. www.univie.ac.at/columbus (accessed March 10, 2020).
- [17] H. Lischka, R. Shepard, R. M. Pitzer, I. Shavitt, M. Dallos, T. Müller, P. G. Szalay, M. Seth, G. S. Kedziora, S. Yabushita, Z. Zhang. *Phys. Chem. Chem. Phys.* **2001**, *3*, 664. <https://doi.org/10.1039/B008063M>.
- [18] H. Lischka, R. Shepard, F. B. Brown, I. Shavitt, *Int. J. Quantum Chem.* **1981**, *20*, 91. <https://doi.org/10.1002/qua.560200810>.
- [19] T. Helgaker, H. J. Aa. Jensen, P. Jørgensen, J. Olsen, K. Ruud, H. Ågren, T. Andersen, K. L. Bak, V. Bakken, O. Christiansen, *et. al.* DALTON, an Ab Initio Electronic Structure Program, Release 1.0. 1997.

- 1
2
3
4
5 [20] T. H. Dunning, *J. Chem. Phys.* **1989**, *90*, 1007. <https://doi.org/10.1063/1.456153>.
6
7 [21] R. A. Kendall, T. H. Dunning, R. J. Harrison, *J. Chem. Phys.* **1992**, *96*, 6796.
8 <https://doi.org/10.1063/1.46256>.
9
10 [22] D. E. Woon, T. H. Dunning. *J. Chem. Phys.* **1993**, *98*, 1358. <https://doi.org/10.1063/1.464303>.
11
12 [23] M. N. R. Ashfold, G. A. King, D. Murdock, M. G. D. Nix, T. A. A. Oliver, A. G. Sage, *Phys.*
13 *Chem. Chem. Phys.* **2010**, *12*, 1218. <https://doi.org/10.1039/B921706A>.
14
15 [24] L. Zhang, D. G. Truhlar, S. Sun, *Phys. Chem. Chem. Phys.* **2018**, *20*, 28144.
16 <https://doi.org/10.1039/C8CP05215H>.
17
18 [25] H. S. You, S. Han, J. S. Lim, S. K. Kim, *J. Phys. Chem. Lett.* **2015**, *6*, 3202.
19 <https://doi.org/10.1021/acs.jpcclett.5b01420>.
20
21 [26] T. S. Venkatesan, S. G. Ramesh, W. Domcke, *J. Chem. Phys.* **2012**, *136*, 174312.
22 <https://doi.org/10.1063/1.4709608>.
23
24 [27] Guang-Shuang-Mu Lin, C. Xie, D. Xie, *J. Phys. Chem. A* **2017**, *121*, 8432.
25 <https://doi.org/10.1021/acs.jpca.7b09070>.
26
27 [28] H. Lischka, D. Nachtigallova, A. J. A. Aquino, P. G. Szalay, F. Plasser, F. B. C. Machado, M.
28 Barbatti, *Chem. Rev.* **2018**, *118*, 7293. <https://doi.org/10.1021/acs.chemrev.8b00244>.
29
30 [29] S.A. do Monte, M. Dallos, T. Müller, H. Lischka, *Collect. Czech. Chem. Commun.* **2003**, *68*, 447.
31 <https://doi.org/10.1135/cccc20030447>.
32
33
34
35
36
37
38
39
40
41
42
43
44
45
46
47
48
49
50
51
52
53
54
55
56
57
58
59
60

New properties of two new thione isomers of thiophenol



A correct description of excited states properties is the first step towards a deep understanding of the photochemistry of compounds. This article show accurate results for some excited states of two new thione isomers of thiophenol, which can help to discriminate between these three species as well to follow spectroscopically their interconversions.

142x172mm (300 x 300 DPI)

Supporting Information

A comparative multi-reference configuration interaction study of the low-lying states of two thione isomers of thiophenol

Filipe Belarmino de Lima,¹ Gessenildo Pereira Rodrigues,² Juracy Regis de Lucena Junior,³
Elizete Ventura,¹ Rui Fausto,⁴ Igor Reva,^{4*} Silmar Andrade do Monte^{1*}

¹Departamento de Química, CCEN, Universidade Federal da Paraíba, 58059-900, João Pessoa, Brazil

²Faculdade Reboúças, 58406-040, Campina Grande, Brazil

³Departamento de Química, Universidade Estadual da Paraíba, 58429-500, Campina Grande, Brazil

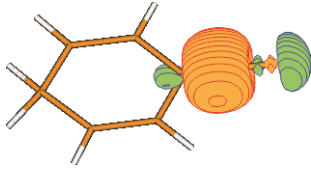
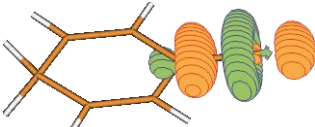
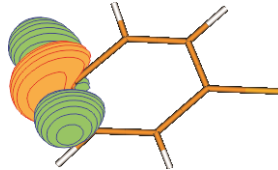
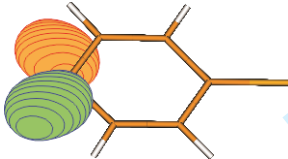
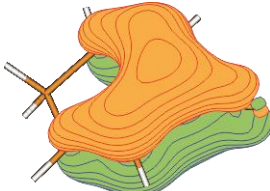
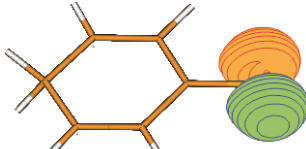
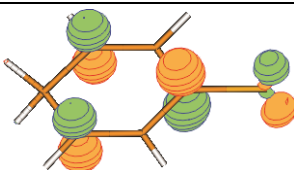
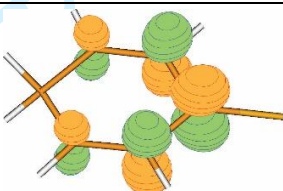
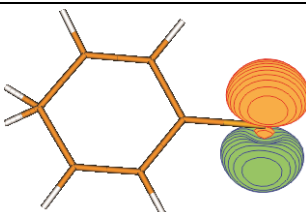
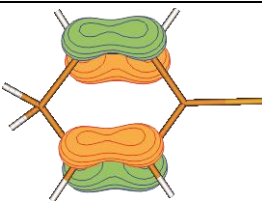
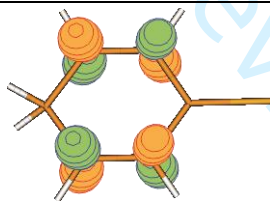
⁴CQC-Departamento de Química, Universidade de Coimbra, 3004-535, Coimbra, Portugal

* Corresponding authors.

e-mails: reva@qui.uc.pt, silmar@quimica.ufpb.br

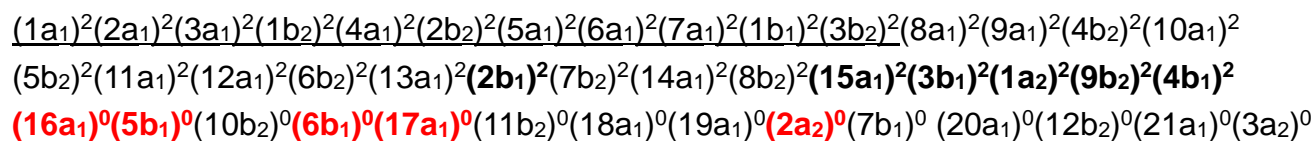
Contents:	Page
Table S1. Active orbitals of Cyclohexa-2,5-diene-1-thione (thione 25)	2
Table S2. Active orbitals of Cyclohexa-2,4-diene-1-thione (thione 24)	3
Occupation numbers of the active orbitals of thiones 25 and 24 , obtained from state-average CASSCF calculations	4
Occupation numbers of the active orbitals of thiones 25 and 24 in the four states, obtained at the <i>w1</i> level	5

Table S1. Active orbitals of Cyclohexa-2,5-diene-1-thione (thione **25**).

Thione 25		
15a ₁ (σ_{CS})	16a ₁ (σ^*_{CS})	17a ₁ (σ^*_{CH})
		
2b ₁ (σ_{CH})	3b ₁ ($\pi_{CS} + \pi_{ring} \equiv \pi_1$)	4b ₁ ($n_{\pi} \equiv \pi_3$)
		
5b ₁ ($\pi^*_{CS} + \pi^*_{ring} \equiv \pi_1^*$)	6b ₁ ($\pi^*_{ring} \equiv \pi_3^*$)	9b ₂ (n)
		
1a ₂ ($\pi_{C=C} \equiv \pi_2$)	2a ₂ ($\pi^*_{C=C} \equiv \pi_2^*$)	
		

Contour values: For the 3b₁ orbital a contour value of 0.05 has been used, while for the remaining orbitals a value of 0.10 has been used.

At the SCF level, the electronic configuration is the following:



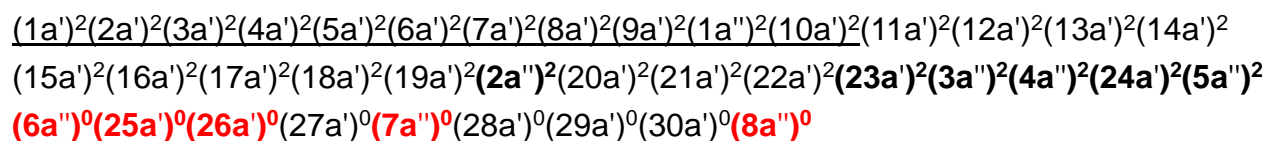
The first eleven (underlined) are core orbitals. The orbitals in **bold** are those included in the CAS space; the active orbitals shown in **black** and **red** correspond to occupied and virtual, respectively.

Table S2. Active orbitals of Cyclohexa-2,4-diene-1-thione (thione **24**).

Thione 24		
23a' (σ_{CS})	24a' (n)	25a' (σ^*_{CS})
26a' (σ^*_{CH})	2a'' (σ_{CH})	3a'' (π_1)
4a'' ($\pi_{CS} \equiv \pi_2$)	5a'' ($\pi_S + \pi_{C=C} \equiv \pi_3$)	6a'' ($\pi_1^*_{ring} + \pi^*_{CS} \equiv \pi_1^*$)
7a'' ($\pi_2^*_{ring} + \pi^*_{CS} \equiv \pi_2^*$)	8a'' ($\pi^*_{C=C} \equiv \pi_3^*$)	

Contour values: For the 5a'', 6a'' and 7a'' orbitals a contour value of 0.05 has been used, while for the remaining orbitals a value of 0.10 has been used.

At the SCF level, the electronic configuration is the following:



The first eleven (underlined) are core orbitals. The orbitals in **bold** are those included in the CAS space; the active orbitals shown in **black** and **red** correspond to occupied and virtual, respectively.

Occupation numbers of the active orbitals obtained from state-average CASSCF calculations (in descending order):

Cyclohexa-2,5-diene-1-thione (thione **25**):

2b ₁	15a ₁	3b ₁	1a ₂	4b ₁	9b ₂	5b ₁	2a ₂	6b ₁	16a ₁	17a ₁
1.9936	1.9775	1.9098	1.6943	1.6978	1.4995	0.7706	0.3405	0.0879	0.0229	0.0055

The last five are anti-bonding orbitals, with occupation numbers smaller than 1.0. The numbering of the π orbitals shown in Table S1 is given according to their occupation numbers. The subscripts in the plots (for instance, CS + ring) refer to the localization of the orbitals.

Cyclohexa-2,4-diene-1-thione (thione **24**):

2a''	23a'	3a''	4a''	5a''	24a'	6a''	7a''	8a''	25a'	26a'
1.9928	1.9759	1.9138	1.8044	1.6046	1.4991	0.7997	0.3019	0.0777	0.0245	0.0056

The last five are anti-bonding orbitals, with occupation numbers smaller than 1.0. The numbering of the π orbitals shown in Table S2 is given according to their occupation numbers. The subscripts in the plots (for instance, S + C=C) refer to the localization of the orbitals.

Occupation numbers of the active orbitals of thiones **25** and **24** in the four states, obtained at the *w1* level.

Cyclohexa-2,5-diene-1-thione (thione **25**):

State	2b ₁	15a ₁	3b ₁	1a ₂	4b ₁	9b ₂	5b ₁	2a ₂	6b ₁	16a ₁	17a ₁
1 ¹ A ₁	1.9834	1.9631	1.9401	1.9186	1.8782	1.9808	0.1391	0.0759	0.0526	0.0386	0.0116
1 ¹ A ₂	1.9839	1.9654	1.9764	1.9138	1.9372	1.0043	1.0031	0.0887	0.0644	0.0351	0.0117
1 ¹ B ₁	1.9825	1.9644	1.9654	1.7520	1.9103	1.0043	0.4527	0.8236	0.0787	0.0352	0.0113
1 ¹ B ₂	1.9828	1.9661	1.9265	1.2977	1.4646	1.9814	0.8783	0.3690	0.0605	0.0350	0.0120

Cyclohexa-2,4-diene-1-thione (thione **24**):

State	2a''	23a'	3a''	4a''	5a''	24a'	6a''	7a''	8a''	25a'	26a'
1 ¹ A'	1.9831	1.9802	1.9404	1.9196	1.8697	1.9625	0.1413	0.0816	0.0514	0.0392	0.0138
1 ¹ A''	1.9839	1.9649	1.9759	1.9413	1.9048	1.0043	1.0023	0.0993	0.0593	0.0354	0.0129
2 ¹ A'	1.9780	1.9713	1.9364	1.9073	1.5330	1.9610	0.4826	0.0995	0.0471	0.0403	0.0171
2 ¹ A''	1.9833	1.9645	1.9701	1.9244	1.6128	1.0043	0.7416	0.6589	0.0723	0.0359	0.01264